A Spontaneously Resoluted Zinc−Organic Framework with Nonlinear Optical and Ferroelectric Properties Generated from Tetrazolate-Ethyl Ester Ligand

Xiao-Qiang Liang,[a] Jiang-Tao Jia,[a] Tao Wu,[b] Dong-Ping Li,[b] Lei Liu,[a] Tsolmon,[a] Guang-Shan Zhu [*a]

[a] *State Key Laboratory of Inorganic Synthesis and Preparative Chemistry, College of Chemistry, Jilin University, Changchun 130012, China*

[b] *State Key Laboratory of Coordination Chemistry, School of Chemistry and Chemical Engineering, Nanjing National Laboratory of Microstructures, Nanjing University, Nanjing 210093, China.*

[*] Corresponding author. Tel.: +86 431 85168331; fax: +86 431 85168589. E-mail address: zhugs@mail. jlu.edu.cn;

General procedures. All other reagents and solvents were commercially available and used without further purification. Elemental analyses for C, H, and N were measured on a CHN-O-Rapid analyzer and an Elementar Vario MICRO analyzer. The IR spectra were performed on a Bruker Vector 22 FT-IR spectrometer by using KBr pellets in the 4000–450 cm^{-1} range. The solid state vibrational circular dichroism (VCD) was obtained on a Bruker PMA50 spectrometer by using KBr pellets in the 1800–1000 cm^{-1} range. Thermogravimetric analyses were collected on a Perkin-Elmer TGA 7 thermogravimetric analyzer from 35 to 800 °C with a heating rate of 20 °C/min in air. The X-ray powder diffraction (XRPD) analysis was performed by a Rigaku diffractometer at a scanning rate of 3º min^{-1} in the 2θ range from 4º to 40º, with graphite monochromatized Cu Kα radiation (λ = 0.15418 nm). The second-order nonlinear optical intensity was estimated by measuring a powder sample relative to urea. A pulsed Q-switched Nd:YAG laser at a wavelength of 1064 nm was used to generate a SHG signal from powder samples. The backscattered SHG light was collected by a spherical concave mirror and passed through a filter that transmits only 532 nm radiation. Electric hysteresis loop of a pellet of powders was measured by the Premier II ferroelectric tester at room temperature.

{$Zn_2(etza)_4$}$_n$ (1) A mixture of $Zn(NO_3)_2 \cdot 6H_2O$ (30 mg, 0.10 mmol), Hetza (31 mg, 0.20 mmol), and 10 mL of $DMF/CH_3CN/H_2O$ (0.5:4.5:5 by volume) was stirred for 0.5h. The colorless diamond-like single crystals of **1** were obtained after it was allowed to stand at room temperature for three weeks. Yield: 40%. Anal. Calc. for $C_{20}H_{28}N_{16}O_8Zn_2$: C, 31.97; H, 3.76; N, 29.83. Found: C, 31.75; H, 3.92; N, 29.52%. IR (KBr, cm^{-1}): 2986(m), 2942(w), 1736(vs), 1709(s), 1651(m), 1558(w), 1539(w), 1513(s), 1472(m), 1434(s), 1398(m), 1376(s), 1335(s), 1212(vs), 1110(m), 1068(m), 1025(s), 939(w), 886(w), 851(w), 792(w), 777(w), 730(w), 677(w).

X-ray Structure Determinations. X-ray intensity data of **1** was collected on a Bruker SMART APEX CCD diffractometer[1] using graphite monochromatized Mo Kα radiation (λ = 0.71073 Å) at 291(2) K. The raw data was reduced and corrected for Lorentz and polarization effect using the SAINT program and for absorption using the SADABS program. The structure was solved by direct methods and refined with the

2

full-matrix least-squares technique using SHELXTL version5.1.[2] Anisotropic thermal parameters were assigned to all non-hydrogen atoms. All hydrogen atoms were placed in calculated positions and refined using a riding model. Selected bond lengths and bond angles are given in Table S1.
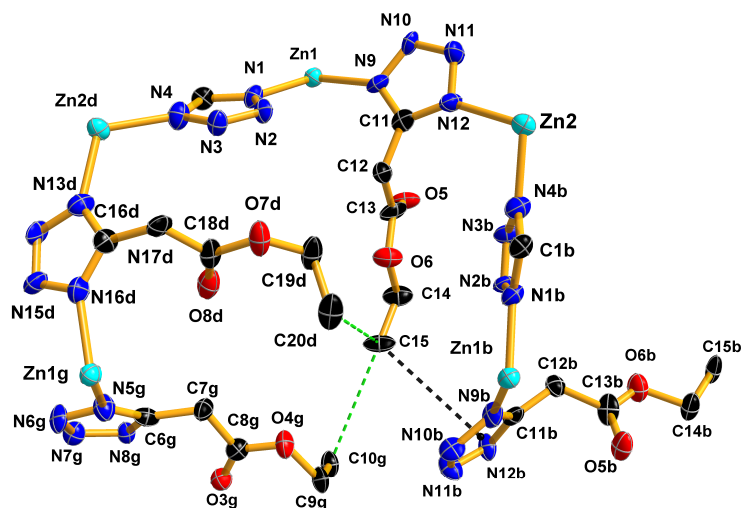
References

1 SMART and SAINT. *Area Detector Control and Integration Software*; Siemens Analytical X-Ray Systems, Inc.: Madison, WI, 1996.

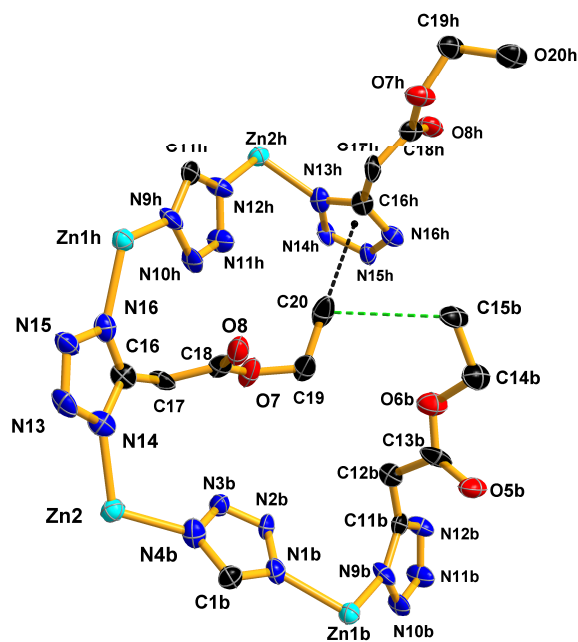2 G. M. Sheldrick, *SHELXTL V5.1 Software Reference Manual*; Bruker AXS, Inc.: Madison, WI, 1997.

Table S1   Selected bond lengths (Å) and angles (°) for **1**

Complex **1**			
Zn(1)−N(1)	2.049(6)	Zn(1)−N(5)	2.026(6)
Zn(1)−N(9)	2.016(7)	Zn(1)−N(16a)	2.044(7)
Zn(2)−N(8c)	2.024(6)	Zn(2)−N(4b)	2.031(7)
Zn(2)−N(13)	2.023(6)	Zn(2)−N(12)	2.099(6)
N(9)−Zn(1)−N(5)	112.7(3)	N(9)−Zn(1)−N(16a)	116.1(3)
N(5)−Zn(1)−N(16a)	104.3(3)	N(9)−Zn(1)−N(1)	107.6(3)
N(5)−Zn(1)−N(1)	107.2(2)	N(16a)−Zn(1)−N(1)	108.6(3)
N(8c)−Zn(2)−N(13)	117.6(2)	N(8c)−Zn(2)−N(4b)	116.3(3)
N(13)−Zn(2)−N(4c)	115.5(3)	N(8c)−Zn(2)−N(12)	97.8(3)
N(13)−Zn(2)−N(12)	99.7(3)	N(4b)−Zn(2)−N(12)	105.4(3)

Symmetry codes : a) −x, y−1/2, −z+1; b) −x, y+1/2, −z+2; c) x−1, y, z for **1**.

(a)

(b)

(c)

(d)

Fig. S1 (a) The first hydrophobic interaction between C5 of alkyl chain and the tetrazolate ring (C1eN1eN2eN3eN4e). (b) The second hydrophobic interaction between C10 of alkyl chain and C15f of alkyl chain. (c) The third hydrophobic interactions between C15 of alkyl chain and C10g, C20d of alkyl chains, and the tetrazolate ring (C11bN1bN2bN3bN4b). (d) The final hydrophobic interactions between C20 of alkyl chain and C15b of alkyl chain, the tetrazolate ring (C16hN13hN14hN15hN16h). Hydrogen atoms and the pendant ester groups of non-existent hydrophobic interactions have been omitted for clarity (Symmetry codes: a) $-x$, $y-1/2$, $-z+1$; b) $x-1$, y, z; c) $-x$, $y+1/2$, $-z+2$; d) $-x$, $y-1/2$, $-z+2$; e) $-x+1$, $y-1/2$, $-z+2$; f) x, y, $-z+1$; g) x, y, $z+1$; h) $-x$, $y+1/2$, $-z+1$.).
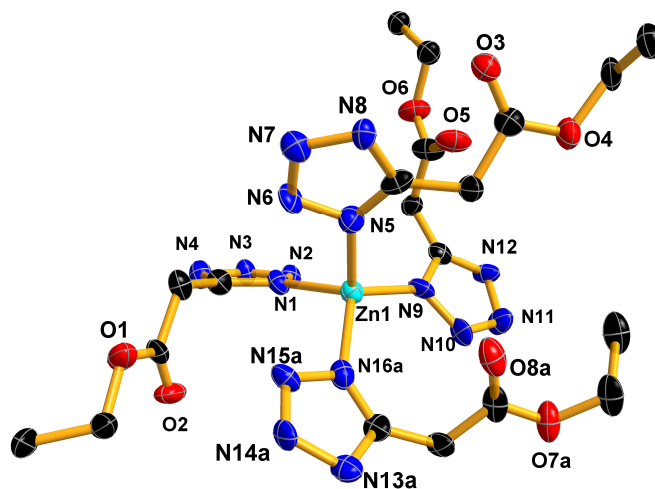
Fig. S2 The zinc coordination geometry of **1** shows chiral configuration (Symmetry code: a) $-x, y-1/2, -z+1$.).
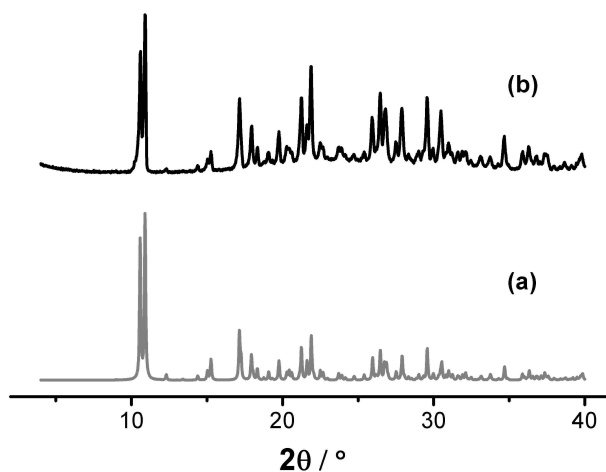

Fig. S3 XRPD patterns of (a) a simulation based on single-crystal analysis of **1**, (b) as-synthesized **1**.
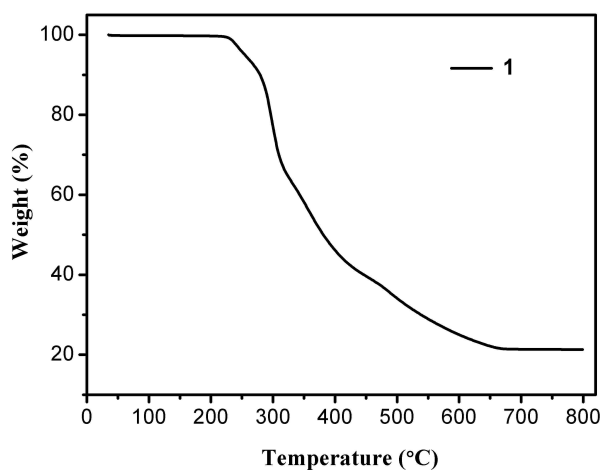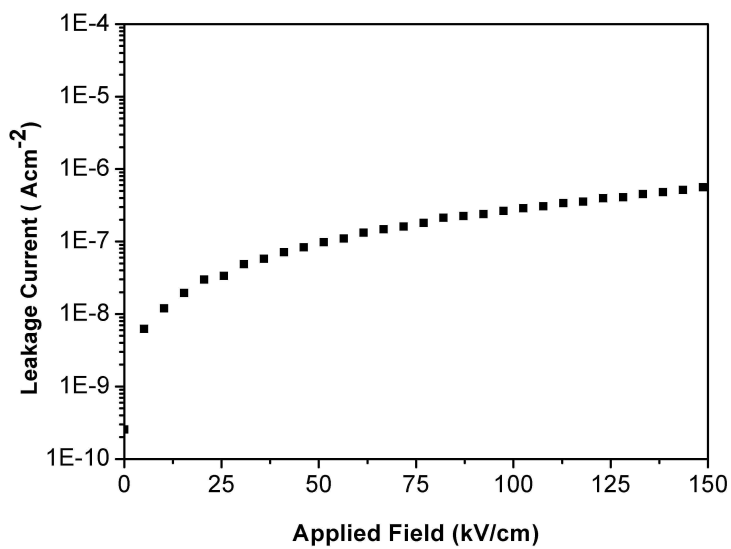
Fig. S4 Thermogravimetric curves for **1**.

Fig. S5 Plot of leakage currents versus electric fields for **1**.